AMERICAN SOCIETY FOR MICROBIOLOGY | Journal of Virology

# Releasing the Genomic RNA Sequestered in the Mumps Virus Nucleocapsid

**Chelsea Severin,[a] James R. Terrell,[a] James R. Zengel,[b] Robert Cox,[c] Richard K. Plemper,[c] Biao He,[b] Ming Luo[a]**

Department of Chemistry[a] and Institute of Biomedical Sciences,[c] Georgia State University, Atlanta, Georgia, USA; Department of Infectious Diseases, College of Veterinary Medicine, University of Georgia, Athens, Georgia, USA[b]

**ABSTRACT**

**In a negative-strand RNA virus, the genomic RNA is sequestered inside the nucleocapsid when the viral RNA-dependent RNA polymerase uses it as the template for viral RNA synthesis. It must require a conformational change in the nucleocapsid protein (N) to make the RNA accessible to the viral polymerase during this process. The structure of an empty mumps virus (MuV) nucleocapsid-like particle was determined to 10.4-Å resolution by cryo-electron microscopy (cryo-EM) image reconstruction. By modeling the crystal structure of parainfluenza virus 5 into the density, it was shown that the α-helix close to the RNA became flexible when RNA was removed. Point mutations in this helix resulted in loss of polymerase activities. Since the core of N is rigid in the nucleocapsid, we suggest that interactions between this region of the mumps virus N and its polymerase, instead of large N domain rotations, lead to exposure of the sequestered genomic RNA.**

**IMPORTANCE**

**Mumps virus (MuV) infection may cause serious diseases, including hearing loss, orchitis, oophoritis, mastitis, and pancreatitis. MuV is a negative-strand RNA virus, similar to rabies virus or Ebola virus, that has a unique mechanism of viral RNA synthesis. They all make their own RNA-dependent RNA polymerase (RdRp). The viral RdRp uses the genomic RNA inside the viral nucleocapsid as the template to synthesize viral RNAs. Since the template RNA is always sequestered in the nucleocapsid, the viral RdRp must find a way to open it up in order to gain access to the covered template. Our work reported here shows that a helix structural element in the MuV nucleocapsid protein becomes open when the sequestered RNA is released. The amino acids related to this helix are required for RdRp to synthesize viral RNA. We propose that the viral RdRp pulls this helix open to release the genomic RNA.**

Many negative-strand RNA viruses (NSVs) are important human pathogens that frequently cause outbreaks. The Ebola virus outbreak in West Africa in 2014 (1) and the pandemic influenza A virus H1N1 outbreak in 2009 (2) are two recent examples. Some pathogens appear to reemerge in spite of available vaccines, such as mumps virus and measles virus (3–5). Effective controls are needed to combat these pathogens. In order to develop more effective countermeasures, the mechanism of NSV replication should be better understood. One of the unique features in NSVs is that the genomic RNA is sequestered in the nucleocapsid (6). During transcription and replication, the viral RNA-dependent RNA polymerase (vRdRp) must be able to gain access to the sequestered genomic RNA in order to use it as the template. For *Rhabdoviridae* and *Paramyxoviridae*, the virus encodes a single nucleocapsid protein (N) that polymerizes as a linear capsid to encapsidate the genomic RNA (7). The viral polymerase complex consists of the large protein (L) and the phosphoprotein (P).

The structure of the nucleocapsid or a nucleocapsid-like particle has been solved for several members of *Rhabdoviridae* and *Paramyxoviridae* by X-ray crystallography or cryo-electron microscopy (cryo-EM) three-dimensional (3D) reconstruction (8–12). The common features among various structures are that the N protein has an N-terminal domain and C-terminal domain in its core, composed mostly of α-helices. When the N subunits assemble into a polymeric capsid, they are aligned in parallel in a linear fashion (13). There are extensive side-by-side interactions between the neighboring domains and domain swaps of extended loops and long termini. The genomic RNA is encapsidated in a cavity formed between the two core domains. Most of the RNA bases are stacked, some of which face the exterior and some the interior of the N protein core. The tight assembly of the nucleocapsid clearly suggests that vRdRp must open the N protein core in order to unveil the genomic RNA. How this action is carried out remains to be discovered. The interaction of the polymerase cofactor P with the nucleocapsid may provide some insights on this subject. The C-terminal domain of vesicular stomatitis virus (VSV) P protein binds between the extended loops in the C-terminal domains of two neighboring parallel N subunits (14). Since the P protein is a part of the vRdRp complex, this binding will place the polymerase in a close proximity to the "gate" covering the genomic RNA. However, the binding of VSV P protein does not seem to induce a significant conformational change in the N protein. It has also been shown that an N-terminal fragment of VSV P protein binds in a truncated empty capsid with an α-helix that sits in the RNA cavity and an extended N-terminal polypeptide that occupies the space vacated by the deletion of the N-ter-

**Received** 15 July 2016 **Accepted** 22 August 2016

**Accepted manuscript posted online** 31 August 2016

**Citation** Severin C, Terrell JR, Zengel JR, Cox R, Plemper RK, He B, Luo M. 2016. Releasing the genomic RNA sequestered in the mumps virus nucleocapsid. J Virol 90:10113–10119. doi:10.1128/JVI.01422-16.

**Editor:** D. S. Lyles, Wake Forest University

Address correspondence to Ming Luo, mluo@gsu.edu.

minal arm of VSV N protein (15). However, this fragment of the VSV P protein could not bind the nucleocapsid or release the genomic RNA. It seems that the P protein can bind the nucleocapsid but is not able to unveil the genomic RNA alone.

Mumps virus (MuV) and parainfluenza virus 5 (PIV5) are members of *Rubulavirus*, a genus of *Paramyxoviridae*. The nucleocapsids of these two viruses tend to coil into a helical structure even when packaged inside the virion. There are on average 13 subunits per turn in the helical structure (16). A unique characteristic of viruses like rubulaviruses is that the length of the RNA genome should be an integer with 6 as a divisor, the so called "rule of six," suggesting that the single N subunit repeat corresponds to a repeat of 6 nucleotides in the encapsidated genomic RNA (17). In previous studies, it was shown that the MuV N protein forms a ring of 13 subunits when it is coexpressed with the P protein in *Escherichia coli* (16). A 78-nucleotide piece of RNA presumably having random sequences was found encapsidated in the ring structure. The packaged RNA could be easily removed by high salt concentrations, low pH, or RNase A, in contrast to the case for VSV nucleocapsid. The C-terminal domain of MuV P protein binds between the two neighboring N subunits in the nucleocapsid, having a similar stoichiometry as VSV P protein. However, the binding site for MuV P protein is closer to the N-terminal domain of its N protein, whereas the binding site for VSV P protein is closer to the C-terminal domain of its N protein. Moreover, the N-terminal domain of MuV P protein also binds and uncoils the nucleocapsid (18). The P N-terminal domain alone can enhance viral RNA synthesis, which has not been reported for other NSVs. Recently, the crystal structure of a truncated PIV5 N-RNA ring was reported (12). The N protein of PIV5 has the same typical two-domain fold as the N protein of other NSVs and is most homologous to that of Nipah virus (NiV) (19). In each N subunit, six nucleotides were covered, with three stacked bases facing the interior and three facing the exterior of the N protein. By comparing the structure of the PIV5 N protein with that of the monomeric NiV N protein, which seems to have a more open conformation between the two N domains, it was hypothesized that the C-terminal domain of PIV5 N protein needs to rotate out in order for the viral polymerase complex to unveil the sequestered RNA (12). In this report, we show that a loop-helix α7 region in MuV N protein is the most flexible region when the sequestered RNA is released. Mutation of a few residues in this region also diminished or reduced viral RNA synthesis. These data suggest an alternative mechanism, namely, that the viral polymerase complex needs only to induce a local conformational change of the loop-helix α7 to unveil the sequestered genomic RNA and does not need to bend open a very stable N protein core.

## MATERIALS AND METHODS

**Expression and purification of recombinant MuV N protein.** All plasmid sequences were based on MuV isolated during an outbreak in Iowa in 2006 (GenBank accession no. JN012242). The coding sequence corresponding to residues 1 to 379 of MuV N protein was coexpressed with the His tagged P protein using plasmid pET28b. After purification of the protein complex with an Ni column, the $N_{379}$ protein was purified by ion-exchange chromatography (HiTrap Q HP; GE Healthcare). The purified $N_{379}$ protein sample that contains random RNA was dialyzed against 20 mM HEPES, pH 7.5. The packaged RNA was removed from the purified $N_{379}$ protein by treatment with 1 mg/ml of RNase A overnight at room temperature.

**Cryo-EM structure of the empty MuV N assembly.** Cryo-EM images of the $N_{379}$-RNA complex and the empty $N_{379}$ complex were collected at the National Resource for Automated Molecular Microscopy (NRAMM) in the Scripps Research Institute. Data were acquired on a Tecnai F20 electron microscope operating at 200 kV, with a Gatan 4kx4k charge-coupled device (CCD) camera to record the images at a pixel size of 1.21 Å. A total of 191 images were included in the final data set for the empty $N_{379}$ complex. Segments of the empty capsid helices were selected with helixboxer from the SPARX/EMAN2 package, using 10% overlap between particles. Particles were aligned using a mask. Contrast transfer function (CTF) corrections were performed with EMAN2. The IHRSR method was used to refine the 3D reconstruction using a noisy cylinder of 220 Å in diameter as the initial model. The initial parameters used for the helical refinement were from the cryo-EM structure of the authentic nucleocapsid (18). The final structure was refined with 5,578 particles, and the resolution was determined to be 10.4 Å using FSC = 0.5. The helical structural model was constructed using PyMol (20) and PIV5 N coordinates from PDB code 4XJN. NiV N coordinates were from PDB code 4CO6. Fitting of the model coordinates into the density was carried out with Chimera (21). Segmentation and superposition of densities were also performed with Chimera.

**Minigenome assays.** The point mutations in the loop-helix α7 region of MuV N were generated by introducing point mutations into the MuV N gene previously cloned into the pCAGGS expression vector (22). Mutations were introduced by splicing by overlap extension (SOE) mutagenesis using Phusion polymerase (Thermo Scientific), as previously described (23). All constructs were confirmed by sequencing at Genewiz.

The minigenome assay was performed as previously described (23). In short, BSR-T7 cells (1 day, 60 to 80% confluent, 24-well plate) were transfected with pCAGGS-P (80 ng), pCAGGS-L (500 ng), pT7-MG-RLuc (100 ng), and pFF-Luc (1 ng), along with various amounts of pCAGGS-N (wild type [wt], Tyr185Pro, Ala197Gln, or Gln200Arg at 25, 50, 100, or 200 ng) using jetPRIME (Polyplus) according to the manufacturer's specifications. After 48 h, cells were lysed and a dual-luciferase assay (Promega) was performed using a portion of the lysate. Luminescence was measuring using a GloMax 96 microplate luminometer (Promega). The ratio of *Renilla* to firefly luciferase was reported for 4 experimental replicates.

Expression levels of N were determined by Western blotting using a portion of the minigenome lysate. All four experimental replicates were combined and mixed with 2× Laemmli sample buffer (Bio-Rad) containing β-mercaptoethanol. Samples were heated at 95°C, resolved on 10% mini-Protean TGX protein gels (Bio-Rad) by SDS-PAGE, and transferred to Amersham Hybond LFP polyvinylidene difluoride (PVDF) membranes (GE Healthcare Life Sciences). Immunoblotting was performed with an anti-N monoclonal antibody (MAb), followed by incubation with a Cy3-conjugated goat anti-mouse IgG (Jackson ImmunoResearch). The blot was visualized on a Typhoon FLA 7000 instrument (GE Healthcare Life Sciences), and densitometry was performed using ImageQuant TL (GE Healthcare). Values were normalized to wt N at 50 ng/well.

## RESULTS

**Structure of a truncated empty capsid.** In a previous study, the MuV N protein was coexpressed with the P protein, and a ring of 13 subunits that packages random RNA inside was isolated (16). When the purified ring was stored for a few weeks at 4°C, it was found that the N protein was truncated after residue 379 ($N_{379}$) (24). The same truncation could be generated by trypsin treatment. Here, a vector was constructed to coexpress $N_{379}$ with the P protein that has a $His_6$ tag at the N terminus. The $N_{379}$-P complex was purified using an Ni column, and the $N_{379}$ protein was further purified with an ion-exchange column. $N_{379}$ still forms a ring of 13 subunits with random RNA packaged. However, the rings of $N_{379}$-RNA can stack and transform into a nucleocapsid-like helical

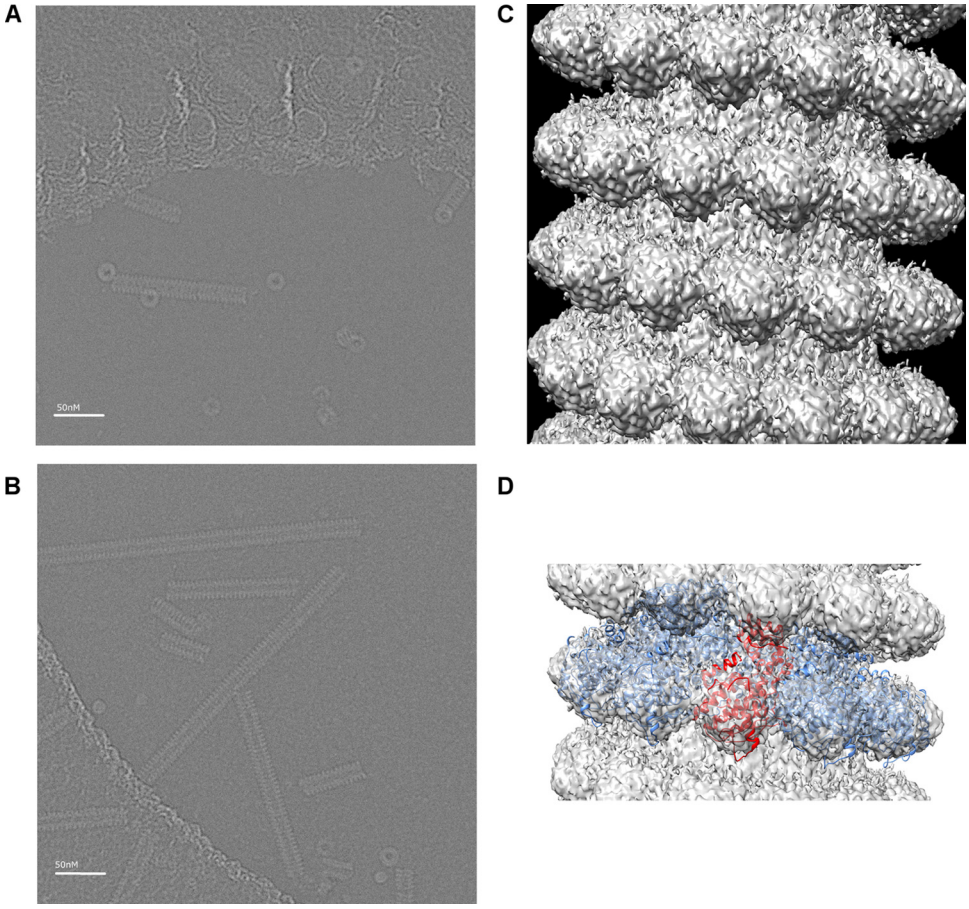


**FIG 1** (A and B) Cryo-EM images of the $N_{379}$-RNA helical structure (A) and the empty $N_{379}$ helical structure (B). Scale bars are 50 nM. (C) The density of the reconstructed empty $N_{379}$ helical structure contoured at 2.0σ level, corresponding roughly to the volume of the model coordinates in panel D. A left-handed helix with four consecutive turns is shown. (D) The structural model constructed with the PIV5 coordinates 4XJN, fitted in the density the empty N helical structure. One turn of 13 subunits is constructed using the coordinates of PIV5 N. The entire turn was fitted into the density as a rigid body (blue ribbons). The electron density is shown by a semitransparent contour. One subunit of the N protein is shown in red.

structure (Fig. 1A). The random RNA sequence could be removed with RNase A, and long helical empty capsids were formed by $N_{379}$ (Fig. 1B). The structure of the empty capsid formed by $N_{379}$ was determined to a 10.4-Å resolution by cryo-EM 3D image reconstruction (Fig. 1C). The diameter of the left-handed truncated empty capsid is about 218 Å, similar to that of the authentic nucleocapsid purified from mumps virions (18). The pitch height, however, is much lower, at about 49 Å (a rise of 3.7 Å per subunit), compared to 67 Å for the authentic nucleocapsid. The rotation of one subunit to the next is 27° about the central axis, making 13.3 subunits per turn, compared to 12.7 subunits per turn in the authentic nucleocapsid. The crystal structure of the PIV5 N-RNA ring complex contains only the fragment of $N_{401}$ (12). Since the sequence of MuV $N_{379}$ is highly homologous to the sequence of $N_{401}$, the coordinates of residues 3 to 379 without RNA from this crystal structure were used to construct an atomic model by rotating a subunit by 27° counterclockwise about the central axis and downshifting by 3.7 Å. The model as a rigid body fits our density map well (Fig. 1D). The empty space between the N- and C-terminal domains of the N protein density is consistent with removal of RNA by RNase A treatment. It appears that transition from a ring structure to a helical structure does not require significant conformational changes in the subunits. In this model, no rotation was introduced in either the N- or C-terminal domain of the N protein.

**Comparison with the authentic nucleocapsid.** The structure of the truncated empty capsid was compared with that of the authentic nucleocapsid determined at an 18-Å resolution (18). The density of the two structures was segmented at about the 2σ contour level. As shown in Fig. 2A, the two segments can be superimposed fairly well except for two regions. The authentic nucleocapsid has more density between the N- and C-terminal domains, consistent with having genomic RNA encapsidated in the nucleocapsid. As shown in Fig. 2B, there is no density corresponding to the location of RNA when the coordinates of PIV5 N are superimposed in the segment. There is also a piece of extra density in the authentic nucleocapsid near the C-terminal end of $N_{379}$. When the density of an $N_{379}$ segment is superimposed onto the helical structure of the authentic nucleocapsid (Fig. 2C), this extra piece of density is involved in the contact between the successive turns. The extra density seems to be responsible for increasing the pitch height of the authentic nucleocapsid. Part of residues 380 to 549, missing from $N_{379}$ (also known as the N-tail), corresponds to this piece of density, but the size of the density is too small to account

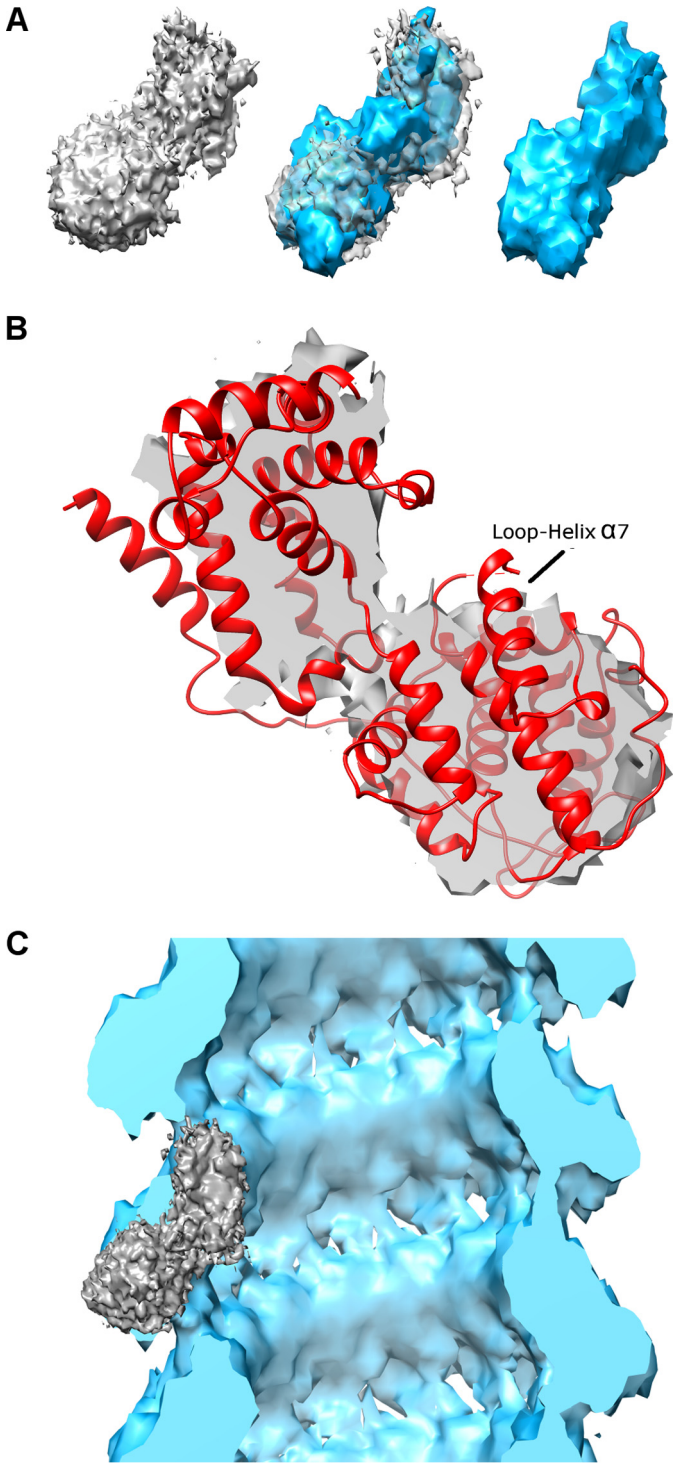


**FIG 2** (A) Superposition (central image) of the segmented density of the empty $N_{379}$ helical structure (transparent gray) with that of the authentic nucleocapsid (cyan). (B) The coordinates of PIV5 N without RNA (red ribbon) were superimposed with the segmented density. Half of the segmented density was removed by slicing through the center. The loop-helix α7 region is labeled. The cleft in the MuV density corresponds to the location where the RNA would be released. (C) Superposition of the segmented density of the empty $N_{379}$ helical structure (gray) with the helical density of the authentic nucleocapsid (cyan). The density of the authentic nucleocapsid is clipped through the center.

for all residues. While some of the N-tail residues make contacts between the successive turns, the rest of the N-tail is likely to point to the exterior of the helical structure, where it was shown to interact with the nucleocapsid binding domain of the P protein (18).

**How is the encapsidated genomic RNA unveiled by the viral polymerase?** As shown for a number of negative-strand RNA virus nucleocapsid-like structures, the genomic RNA is sequestered in the nucleocapsid with some of the stacked nucleotide bases facing the interior of the N protein (25). In order to use the sequestered genomic RNA as a template for viral synthesis, a conformational change must be induced by the viral polymerase complex to temporarily release the RNA from the N protein. It has been suggested that one of the two N protein domains surrounding the genomic RNA can swing open so the template RNA becomes accessible by vRdRp (12). The N structure from the PIV5 $N_{401}$-RNA complex was compared with that of a truncated N protein ($N_{32–383}$) of NiV in complex with a fragment of the P protein. There is no RNA in the NiV $N_{32–383}$ structure. The comparison showed that the N- or C-terminal domain of the two N proteins can be superimposed separately. If the N-terminal domains were superimposed, it would require a 20° rotation to bring the C-terminal domain of PIV5 N to overlap that of NiV N. This observation was the basis for the hypothesis that the C-terminal domain of PIV5 N is the domain that rotates upon polymerase binding, not the N-terminal domain (12). To examine this hypothesis, the coordinates of PIV5 N and NiV $N_{32–383}$ were superimposed onto the density of the truncated empty capsid of MuV. The PIV5 N structure can be superimposed well without any conformational changes in the two domains. On the other hand, only one of the two domains in NiV $N_{32–383}$ may be properly superimposed in the density each time. If the N-terminal domain is superimposed, the C-terminal domain of NiV $N_{32–383}$ will stick out of the density toward the interior of the helical empty capsid. If the C-terminal domain is superimposed, the N-terminal domain of NiV $N_{32–383}$ will be outside density. However, the motion that may bring the N-terminal domain back into the density requires mostly a rotation about the helical axis (Fig. 3C). The two sets of coordinates were also mapped based on the B factor, a factor that correlates with structural stability (Fig. 3A and D). The core of the PIV5 N-RNA complex has very low B factors, suggesting a high structural stability. This will make it very hard to open either the C- or N-terminal domain because of the high energy requirement. Similarly, the core of NiV $N_{32–383}$ also has lower B factors. However, the surface residues in the N-terminal domain NiV $N_{32–383}$ have relatively higher B factors. This is consistent with the fact that the truncated monomeric NiV N protein has neither neighboring subunits nor RNA to stabilize it. It was also observed that when the RNA was removed from the authentic nucleocapsid, the MuV empty capsid became more flexible (18). We noticed, however, that residues in helix α7 and the prior loop of PIV5 N also have very high B factors comparable to the residues in the N and C termini, among which residues 183 to 186 were actually disordered (Fig. 3B). The homologous region in the NiV N has similar B factors and disordered residues. When the coordinates of PIV5 N are superimposed with the structure of the MuV truncated empty capsid, there is no density corresponding to the loop-helix α7 (Fig. 2B). The same observation was made with superposition of the NiV $N_{32–383}$, in which there is no corresponding density for the homologous loop-helix. We propose that the viral polymerase

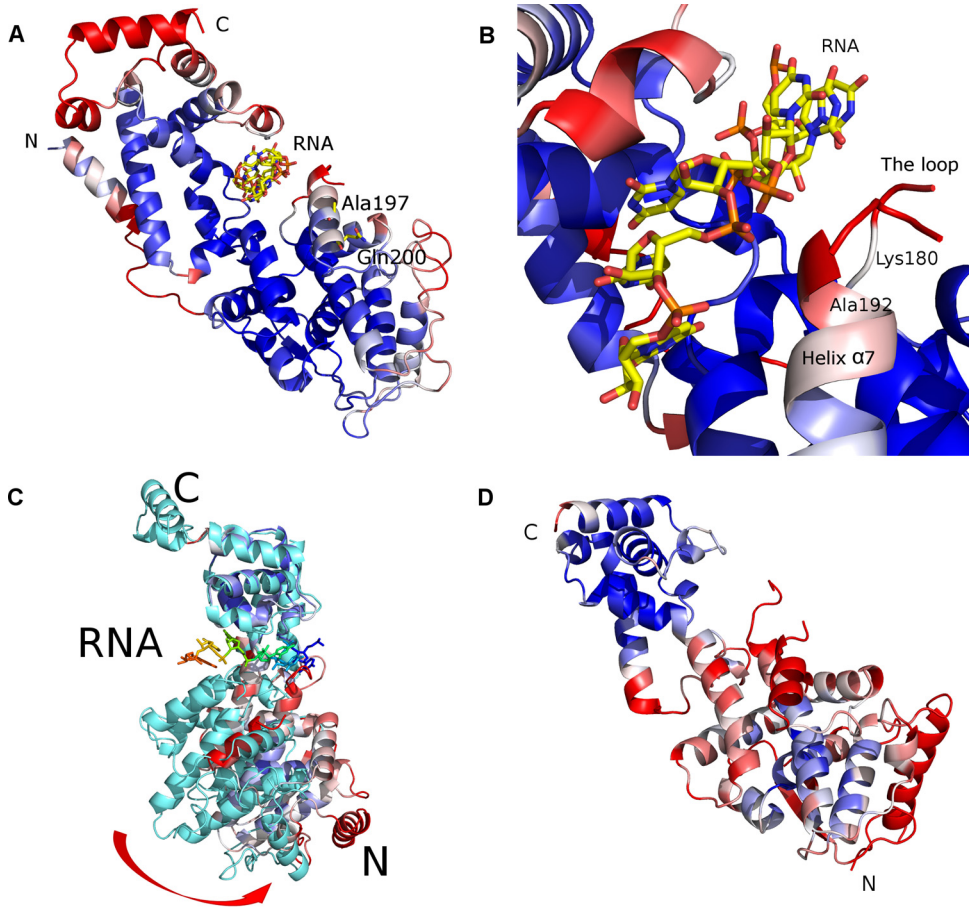


**FIG 3** (A) Ribbon drawing of the PIV5 N structure (4XJN) colored by the B factor (side view). The blue color corresponds to a low B factor, whereas the red color corresponds to a high B factor. N and C, N terminus and C terminus, respectively, of the PIV5 N-RNA complex. The encapsidated RNA is shown for one N subunit as a stick model. Residues Ala197 and Gln200 are displayed as sticks and labeled. Residue Tyr185 is not present in the crystal structure. (B) A close-up view of helix α7 and the loop prior to helix α7 in the PIV5 N structure. Residues Lys180 and Ala192 are at each end of this flexible region. Disordered residues183 to 186 are not present. (C) Ribbon drawings to illustrate the motion required to fit the coordinates of NiV N (PDB code 4CO6) with the density of the empty $N_{379}$ helical complex. The structure of NiV N is represented by a ribbon in cyan. The structure of PIV5 N as fitted in the density of the empty $N_{379}$ helical complex is represented by a ribbon colored from blue to red by B factors. The view is approximately down the axis of the empty $N_{379}$ helical complex. The C-terminal domains of the two structures were superimposed together. The red arrow indicates the rotational motion required for the N-terminal domain of NiV N to be superimposed with that of PIV5 N. N and C, N and C termini of PIV5 N, respectively. RNA is encapsidated in the center of PIV5 N. (D) Ribbon drawing of the NiV N structure colored by the B factor (side view). The blue color corresponds to a low B factor, whereas the red color corresponds to a high B factor. N and C, N terminus and C terminus, respectively.

complex is required only to open this loop-helix α7 region in order to gain access to the sequestered RNA, instead of bending open a very stable protein core by rotating either the N- or C-terminal domain.

**Residues in the loop-helix α7 are critical.** We compared the sequence of the MuV N protein with that of the PIV5 N protein and found that in the loop-helix α7, three residues are different between the two proteins: residues Tyr185, Ala197, and Gln200 (Fig. 3A). Since vRdRp of one virus could not work with other nucleocapsids, we argue that changing these three amino acids of MuV to those of PIV5 would compromise viral RNA synthesis if they are required for vRdRp interactions with the N protein. Three mutant N proteins were therefore generated, corresponding to the changes Tyr185Pro, Ala197Gln, and Gln200Arg. The minigenome activity assay and Western blotting for quantitating the expression of mutant MuV N proteins were carried out, and the results are summarized in Fig. 4. According to Western blot analysis, the mutant N proteins have levels of expression similar to or even higher than that of the wt sequence (Fig. 4A). However, the minigenome activities using the mutant N proteins were significantly reduced compared to that using the wt N protein (Fig. 4B). Gln200Arg had almost no activity, consistent with the fact that mutation from Gln to Arg represents a large side chain change from a polar residue to a positively charged residue.

## DISCUSSION

Transition of the MuV N-RNA complex to a helical structure suggests that the helical nucleocapsid is a very stable structure. By changing to a helical structure, most of the lateral interactions observed in the N-RNA ring are likely to be preserved, especially if the N subunit is allowed to rotate itself. The interactions observed in the crystal structure of NSV N-RNA rings are therefore valid for interpreting N subunit interactions in the authentic nucleocapsid. The protein-protein contact between the neighboring N subunits

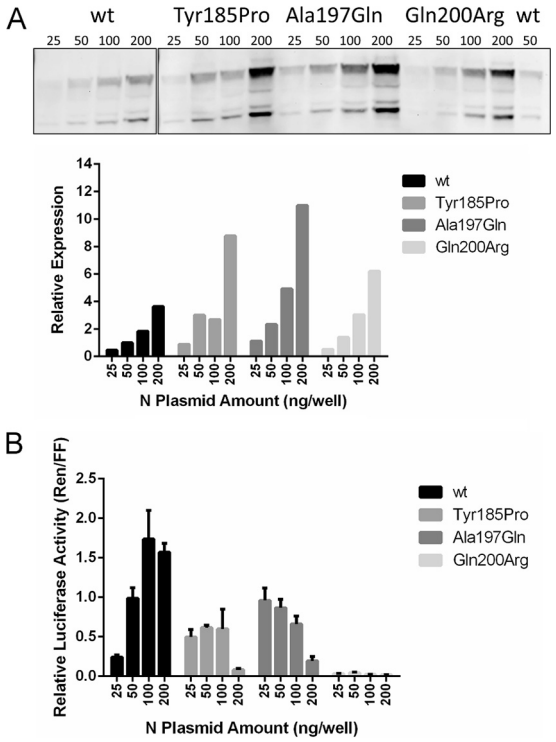


**FIG 4** (A) Expression levels of the mutated MuV N proteins detected by Western blotting, compared with that of wt MuV N. The full-length N protein was used for quantitation. (B) Activities of the minigenome reporter gene when the mutated MuV N proteins were used in the system. wt MuV N was used as the positive control.

is massive in the nucleocapsid, provided by side-by-side interactions and domain swaps. Deletion of these interactions will result in disassembly of the capsid and loss of RNA encapsidation (26). In the structure of empty capsids shown here and reported previously (26), the same interactions are retained, suggesting that release of sequestered RNA may not require global conformational changes in the N protein. As shown in the PIV5 N-RNA structure, each C-terminal domain has an interface of 327 Å$^2$ with both sides and domain swapping of its C-terminal arm (residues 373 to 401) with another neighboring N subunit. The interactions of the N-terminal domain are even more extensive (883 Å$^2$). A global conformational change of either domain will cost a large amount of destabilization energy. In addition, the integrity of the nucleocapsid must be restored when the viral polymerase finishes RNA synthesis at the region where RNA is unveiled. It may not be reversible if large conformational changes are induced in the N protein during viral RNA synthesis.

The conformation of the two domains in NiV N appears to be more open than that in the N protein of respiratory syncytial virus (19). However, the two N domains may become more closed in other NSV N proteins, such as bunyaviruses (27–30). The degree of openness of the two domains may not necessarily be related to the mode of RNA encapsidation by the N protein or the flexibility of the N protein core. If a hinge is present between the two N domains, it is likely that a more flexible linker is present in the N protein core. Based on the B factors, there is no such flexible linker between the two domains in either PIV5 or NiV N. Moreover, the crystal structure of a measles virus Ncore-P complex shows that the RNA-free monomeric N protein has a more collapsed conformation than that in the nucleocapsid (31). The conformation of the RNA-free N protein is therefore not related to how the sequestered RNA is unveiled during viral RNA synthesis.

An N-terminal fragment of NiV P could bind the RNA-free monomeric truncated $N_{32–383}$, but no evidence supports that this fragment could bind the nucleocapsid (19). The P protein functions as a chaperone to keep the N protein monomeric before nucleocapsid assembly. The published structures showed that the N-terminal regions can bind at the sites that are involved in stabilizing the nucleocapsid, such as interactions for domain swapping or RNA binding (19, 31). Once the monomeric N subunit is incorporated in the nucleocapsid, the P protein must be dissociated, and the interactions of the N subunits are established. There is no evidence to suggest that the P protein can compete with such cooperative interactions. Our results showed that the loop-helix α7 is the most flexible region when sequestered RNA is released. When RNA is removed, this region becomes more flexible. Single-amino-acid mutations of the MuV N sequence to those of the PIV5 N sequence significantly reduced the minigenome activity (Fig. 4), reaffirming the involvement of this region in viral RNA synthesis. We suggest that specific interactions of this MuV N region with the polymerase are required for unveiling the RNA for viral RNA synthesis. These observations are consistent with the proposed mechanism that the viral polymerase complex can unveil the sequestered RNA by inducing a local conformational change of the loop-helix α7. The loop-helix α7 should be able to readily restore the structure of the nucleocapsid after viral RNA synthesis because it is only a local conformational change.

## ACKNOWLEDGMENTS

We thank Ingeborg Schmidt-Krey for suggestions. We thank the staff at the National Resource for Automated Molecular Microscopy for their assistance with cryo-EM image collections.

Some of the work presented here was conducted at the National Resource for Automated Molecular Microscopy, which is supported by a grant from the National Institute of General Medical Sciences (9 P41 GM103310) of the National Institutes of Health.

## FUNDING INFORMATION

This work, including the efforts of Ming Luo, was funded by HHS | NIH | National Institute of Allergy and Infectious Diseases (NIAID) (AI106307).

## REFERENCES

1. **Green A.** 2014. West Africa struggles to contain Ebola outbreak. Lancet **383:**1196. http://dx.doi.org/10.1016/S0140-6736(14)60579-1.
2. **Shinde V, Bridges CB, Uyeki TM, Shu B, Balish A, Xu X, Lindstrom S, Gubareva LV, Deyde V, Garten RJ, Harris M, Gerber S, Vagasky S, Smith F, Pascoe N, Martin K, Dufficy D, Ritger K, Conover C, Quinlisk P, Klimov A, Bresee JS, Finelli L.** 2009. Triple-reassortant swine influenza A (H1) in humans in the United States, 2005–2009. N Engl J Med **360:**2616–2625. http://dx.doi.org/10.1056/NEJMoa0903812.
3. **Centers for Disease C, Prevention.** 2006. Mumps outbreak at a summer camp—New York, 2005. MMWR Morb Mortal Wkly Rep **55:**175–177.
4. **Rota JS, Rosen JB, Doll MK, McNall RJ, McGrew M, Williams N, Lopareva EN, Barskey AE, Punsalang A, Jr, Rota PA, Oleszko WR, Hickman CJ, Zimmerman CM, Bellini WJ.** 2013. Comparison of the sensitivity of laboratory diagnostic methods from a well-characterized outbreak of mumps in New York city in 2009. Clin Vaccine Immunol **20:**391–396. http://dx.doi.org/10.1128/CVI.00660-12.
5. **Zipprich J, Winter K, Hacker J, Xia D, Watt J, Harriman K, Centers for Disease C, Prevention.** 2015. Measles outbreak—California, December 2014-February 2015. MMWR Morb Mortal Wkly Rep **64:**153–154.

6. **Luo M.** 2011. Negative strand RNA virus. World Scientific, Singapore.
7. **Ivanov I, Yabukarski F, Ruigrok RW, Jamin M.** 2011. Structural insights into the rhabdovirus transcription/replication complex. Virus Res **162:** 126–137. http://dx.doi.org/10.1016/j.virusres.2011.09.025.
8. **Green TJ, Zhang X, Wertz GW, Luo M.** 2006. Structure of the vesicular stomatitis virus nucleoprotein-RNA complex. Science **313:**357–360. http://dx.doi.org/10.1126/science.1126953.
9. **Albertini AA, Wernimont AK, Muziol T, Ravelli RB, Clapier CR, Schoehn G, Weissenhorn W, Ruigrok RW.** 2006. Crystal structure of the rabies virus nucleoprotein-RNA complex. Science **313:**360–363. http://dx.doi.org/10.1126/science.1125280.
10. **Tawar RG, Duquerroy S, Vonrhein C, Varela PF, Damier-Piolle L, Castagne N, MacLellan K, Bedouelle H, Bricogne G, Bhella D, Eleouet JF, Rey FA.** 2009. Crystal structure of a nucleocapsid-like nucleoprotein-RNA complex of respiratory syncytial virus. Science **326:**1279–1283. http://dx.doi.org/10.1126/science.1177634.
11. **Gutsche I, Desfosses A, Effantin G, Ling WL, Haupt M, Ruigrok RW, Sachse C, Schoehn G.** 2015. Structural virology. Near-atomic cryo-EM structure of the helical measles virus nucleocapsid. Science **348:**704–707. http://dx.doi.org/10.1126/science.aaa5137.
12. **Alayyoubi M, Leser GP, Kors CA, Lamb RA.** 2015. Structure of the paramyxovirus parainfluenza virus 5 nucleoprotein-RNA complex. Proc Natl Acad Sci U S A **112:**E1792–E1799. http://dx.doi.org/10.1073/pnas.1503941112.
13. **Green TJ, Cox R, Tsao J, Rowse M, Qiu S, Luo M.** 2014. Common mechanism for RNA encapsidation by negative-strand RNA viruses. J Virol **88:**3766–3775. http://dx.doi.org/10.1128/JVI.03483-13.
14. **Green TJ, Luo M.** 2009. Structure of the vesicular stomatitis virus nucleocapsid in complex with the nucleocapsid-binding domain of the small polymerase cofactor, P. Proc Natl Acad Sci U S A **106:**11713–11718. http://dx.doi.org/10.1073/pnas.0903228106.
15. **Leyrat C, Yabukarski F, Tarbouriech N, Ribeiro EA, Jr, Jensen MR, Blackledge M, Ruigrok RW, Jamin M.** 2011. Structure of the vesicular stomatitis virus $N^0$-P complex. PLoS Pathog **7:**e1002248. http://dx.doi.org/10.1371/journal.ppat.1002248.
16. **Cox R, Green TJ, Qiu S, Kang J, Tsao J, Prevelige PE, He B, Luo M.** 2009. Characterization of a mumps virus nucleocapsidlike particle. J Virol **83:**11402–11406. http://dx.doi.org/10.1128/JVI.00504-09.
17. **Vulliemoz D, Roux L.** 2001. "Rule of six": how does the Sendai virus RNA polymerase keep count? J Virol **75:**4506–4518. http://dx.doi.org/10.1128/JVI.75.10.4506-4518.2001.
18. **Cox R, Pickar A, Qiu S, Tsao J, Rodenburg C, Dokland T, Elson A, He B, Luo M.** 2014. Structural studies on the authentic mumps virus nucleocapsid showing uncoiling by the phosphoprotein. Proc Natl Acad Sci U S A **111:**15208–15213. http://dx.doi.org/10.1073/pnas.1413268111.
19. **Yabukarski F, Lawrence P, Tarbouriech N, Bourhis JM, Delaforge E, Jensen MR, Ruigrok RW, Blackledge M, Volchkov V, Jamin M.** 2014. Structure of Nipah virus unassembled nucleoprotein in complex with its viral chaperone. Nat Struct Mol Biol **21:**754–759. http://dx.doi.org/10.1038/nsmb.2868.
20. **PyMol.** The PyMOL molecular graphics system, version 1.3. Schrödinger, LLC, Cambridge, MA.
21. **Pettersen EF, Goddard TD, Huang CC, Couch GS, Greenblatt DM, Meng EC, Ferrin TE.** 2004. UCSF Chimera—a visualization system for exploratory research and analysis. J Comput Chem **25:**1605–1612. http://dx.doi.org/10.1002/jcc.20084.
22. **Xu P, Li Z, Sun D, Lin Y, Wu J, Rota PA, He B.** 2011. Rescue of wild-type mumps virus from a strain associated with recent outbreaks helps to define the role of the SH ORF in the pathogenesis of mumps virus. Virology **417:**126–136. http://dx.doi.org/10.1016/j.virol.2011.05.003.
23. **Pickar A, Xu P, Elson A, Li Z, Zengel J, He B.** 2014. Roles of serine and threonine residues of mumps virus P protein in viral transcription and replication. J Virol **88:**4414–4422. http://dx.doi.org/10.1128/JVI.03673-13.
24. **Cox R, Green TJ, Purushotham S, Deivanayagam C, Bedwell GJ, Prevelige PE, Luo M.** 2013. Structural and functional characterization of the mumps virus phosphoprotein. J Virol **87:**7558–7568. http://dx.doi.org/10.1128/JVI.00653-13.
25. **Green TJ, Rowse M, Tsao J, Kang J, Ge P, Zhou ZH, Luo M.** 2011. Access to RNA encapsidated in the nucleocapsid of vesicular stomatitis virus. J Virol **85:**2714–2722. http://dx.doi.org/10.1128/JVI.01927-10.
26. **Zhang X, Green TJ, Tsao J, Qiu S, Luo M.** 2008. Role of intermolecular interactions of vesicular stomatitis virus nucleoprotein in RNA encapsidation. J Virol **82:**674–682. http://dx.doi.org/10.1128/JVI.00935-07.
27. **Dong H, Li P, Bottcher B, Elliott RM, Dong C.** 2013. Crystal structure of Schmallenberg orthobunyavirus nucleoprotein-RNA complex reveals a novel RNA sequestration mechanism. Rna **19:**1129–1136. http://dx.doi.org/10.1261/rna.039057.113.
28. **Niu F, Shaw N, Wang YE, Jiao L, Ding W, Li X, Zhu P, Upur H, Ouyang S, Cheng G, Liu ZJ.** 2013. Structure of the Leanyer orthobunyavirus nucleoprotein-RNA complex reveals unique architecture for RNA encapsidation. Proc Natl Acad Sci U S A **110:**9054–9059. http://dx.doi.org/10.1073/pnas.1300035110.
29. **Reguera J, Malet H, Weber F, Cusack S.** 2013. Structural basis for encapsidation of genomic RNA by La Crosse orthobunyavirus nucleoprotein. Proc Natl Acad Sci U S A **110:**7246–7251. http://dx.doi.org/10.1073/pnas.1302298110.
30. **Ariza A, Tanner SJ, Walter CT, Dent KC, Shepherd DA, Wu W, Matthews SV, Hiscox JA, Green TJ, Luo M, Elliott RM, Fooks AR, Ashcroft AE, Stonehouse NJ, Ranson NA, Barr JN, Edwards TA.** 2013. Nucleocapsid protein structures from orthobunyaviruses reveal insight into ribonucleoprotein architecture and RNA polymerization. Nucleic Acids Res **41:**5912–5926. http://dx.doi.org/10.1093/nar/gkt268.
31. **Guryanov SG, Liljeroos L, Kasaragod P, Kajander T, Butcher SJ.** 2016. Crystal structure of the measles virus nucleoprotein core in complex with an N-terminal region of phosphoprotein. J Virol **90:**2849–2857. http://dx.doi.org/10.1128/JVI.02865-15.